Low-Cost Comb-Line-Fed Microstrip Antenna Arrays with Low Sidelobe Level for 77 GHz Automotive Radar Applications

Soheil Yasini, Karim Mohammadpour-Aghdam[*], and Mahmoud Mohammad-Taheri

Abstract—In this paper, we design and fabricate a side lobe comb-line fed microstrip antenna array at the frequency of 77 GHz. This antenna can be used in car and also in peripheral protection radars. To design the antenna, a radiating microstrip element on a simple sublayer is first designed and optimized in order to have desirable specification at 77 GHz. Secondly, a one-dimensional array is formed using a row of microstrip antenna array with 32 serried elements. Finally, a two-dimensional antenna array with 16 rows is fabricated and subsequently fed with a waveguide to complete the antenna design.

1. INTRODUCTION

Many researchers have reported the methods to design and implement a low side lobe microstrip antenna array with comb-line feeding [1–10, 15]. However, any method has its own advantages and disadvantages. Some methods use an equivalent circuit for series elements and assign voltage amplitude to each element [1–3, 5, 6, 9, 10]. Others, such as [4], use a power divider in order to obtain the appropriate amplitudes associated with each element. Some of them have used series [1, 3, 5] or parallel [9] microstrip feed line for equivalent circuit while others have used waveguide-slot-microstrip feed [2, 7, 8, 10]. Many of the designers have suggested solutions in order to optimize the size of the antenna by reducing the total number of the antenna elements [15], while others have focused on reducing the side lobe level in the radiation pattern [3, 5]. The designed antennas by the above methods are implemented in Automotive Radars [1, 2, 4], peripheral protection radars, while others have been used in industrial applications.

The 77 GHz fabricated comb-line fed antenna array in this paper which has a wideband and low side lobe with optimum resolution will be used in collision avoidance radar. Because of the mentioned characteristics, the targets can be detected with a minimum error.

2. DESIGN OF ARRAY ELEMENT

Radiation element of the antenna array should resonate at frequency of 77 GHz. The substrate of the antenna is Rogers RO4003, with the permittivity, loss tangent, and thickness of 3.55, 0.0027, and 0.2032 mm, respectively. The metal used in the substrate is copper with the thickness of 17 μm. Antenna array element is shown in Figure 1.

The initial values of the patch width (W) and length (L) are equal to 0.937 mm, which corresponds to the resonant frequency of 77 GHz [1].

To find the input impedance of the antenna element, we should model the effect of coupling. Thus, we place the element between four other elements in such a way that the distance between the adjacent elements is $\lambda_g/2$. Full-wave simulation shows that the input impedance of the element at the resonance frequency is 584 Ω [1].
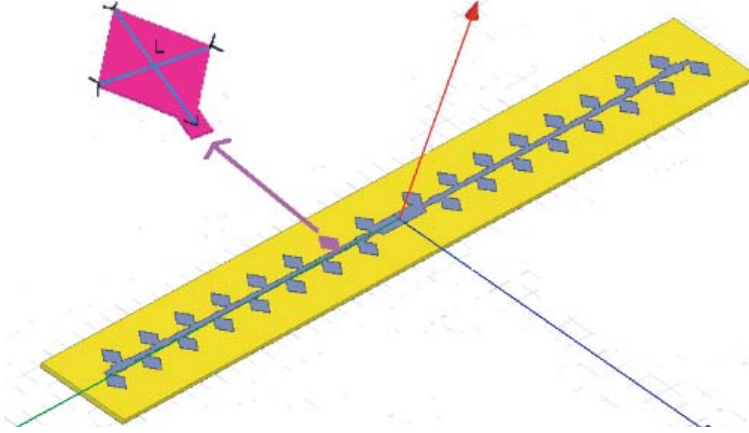
Figure 1. Single in line antenna array with 32 elements.

3. DESIGN OF SINGLE-LINE ANTENNA ARRAY

To design a single-line antenna array with desirable side lobe level of better than -20 dB, the values of the power reaching each element should be weighted. Using Chebyshev weighting coefficient, voltage amplitude of each element has been computed. For weighting, we should determine the distance between each element and the adjacent element. To achieve a broad side radiation pattern, the wave phase difference between the adjacent elements should be equal to 360 degrees. For reducing the distance between adjacent elements, the phase difference generated by the transmission line inserted between adjacent elements should be equal to 180 degrees, and each element should be in reverse direction with respect to the element prior it in order to obtain $180°$ positional phase difference. If we assume that the current reaching the first element is equal to 1 A, then the current reaching the second element is n_1 times bigger, and current reaching the $(i+1)$th element is $n_1 \times n_2 \times \ldots \times n_i$ times bigger than that of the first element. The value of n_i is expressed as [1]:

$$n_i = Z_{2i}/Z_{2i-1} \tag{1}$$

where Z_{2i} and Z_{2i-1} are characteristic impedances of the $(2i)$th transmission line and $(2i-1)$th transmission line, respectively.

Having n_i we can calculate the impedance and therefore the length and width of each transmission line. Figure 1 shows the single in-line antenna array [1].

The impedance of the single-line antenna seen at the middle of the antenna and at the frequency of 77.4 GHz should be high enough so that the transmitted power in 2-dimensional antenna array can be transmitted to other rows. For the impedance of single in line antenna array of $143\,\Omega$, the distance between the first adjacent elements is equal to 3.06 mm, greater than 1.12 mm, which is the distance between the second adjacent elements. So the element spacing is nonuniform, and we should use the nonuniform weighting.

In nonuniform weighting, the spacings between adjacent elements are not the same. In this case, the antenna gain is expressed as a function of element spacing and weighting coefficients. The element spacing and weighting coefficients are adjusted in such a way that the minimum error and side lobe level are obtained, and the antenna gain is desirable. By this algorithm the element spacings and weighting coefficients are obtained.

With the nonuniform weighting, the desirable side lobe level will be acquired, and with a similar method, the impedances and in turn the length and width of transmission lines will be obtained. Figure 2 shows the simulated result of radiation pattern of single in line antenna obtained by HFSS. As can be seen in this figure, the side lobe level in the H-plane is -22.2 dB [1], and due to small ground plane, the front to back ratio is 14.2 dB.
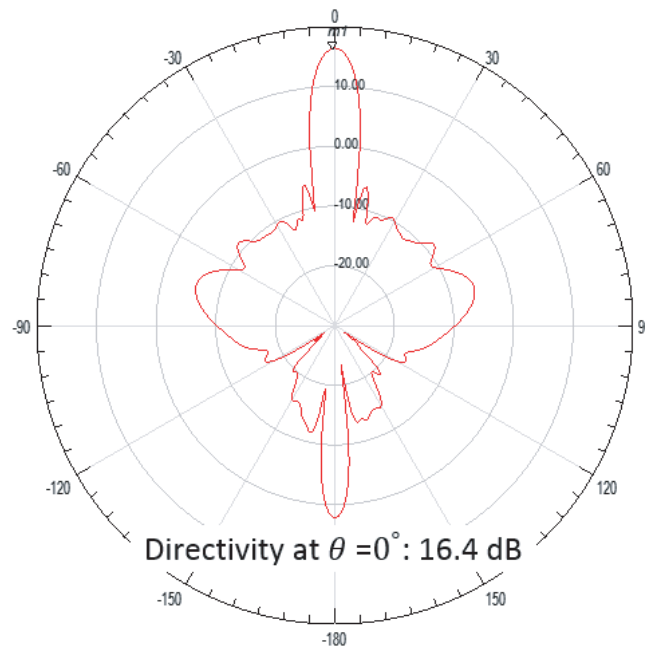
Figure 2. The single-line antenna directivity in plane of $\varphi = 0°$.

4. TWO-DIMENSIONAL ANTENNA ARRAY

After the design of the one-dimensional antenna array, we design a two-dimensional antenna array. In this design procedure, the one-dimensional array is called a row, then the rows are serially placed, and the cross lines are fed from the middle of the rows. As the elements of each row should not touch to the second row, the distance between two adjacent rows cannot be equal to $\lambda_g/2$. Therefore, the distance between adjacent rows is chosen to be equal to λ_g, and two transmission lines between adjacent rows are increased to four with the length of $\lambda_g/4$ where the second, third, and fourth transmission lines have the same impedance, length, and width. Having the new weightings ratio, n_i, we can calculate the impedance, length, and width of each transmission line. The final antenna array has 16 rows. By choosing the distance between two middle rows to λ_g, weighting is uniform, and we can use the Chebyshev weighting factor as well. The antenna's dimensions are $4.2 \, \text{cm} \times 4.2 \, \text{cm}$. The radiation patterns of the final design in H and E planes have been obtained by full-wave simulator and are shown in Figure 3. As can be seen from this figure, the side lobe levels in H- and E-planes are $-15.6 \, \text{dB}$ and $-17 \, \text{dB}$, respectively [1].

5. ANTENNA FEED DESIGN

There is no any practically usable connector feed in $77 \, \text{GHz}$ band in market. So, we have to choose a waveguide connector which is available in millimeter wave band and can be easily matched to the input impedance. So far, there are many waveguide to microstrip transition designs [11–14]. In our design, there is no any via which increases the side lobe level. However, this facilitates the integration with the two-dimensional microstrip antenna array. Figure 4 shows the waveguide to microstrip transition which acts as a matching element.

In fact, a matching element is an element inserted in a waveguide to microstrip transition in which one can adjust the scattering parameters by changing the shape and dimension of this element.

For the waveguide feed design, WR-12 waveguide has been chosen whose frequency band is between 75 and $100 \, \text{GHz}$, and its input impedance is $300 \, \Omega$. For transition design, feed line should be cut at two first rows. Then, the R-L-C impedance as an S2p file from the cut points should be read and modeled
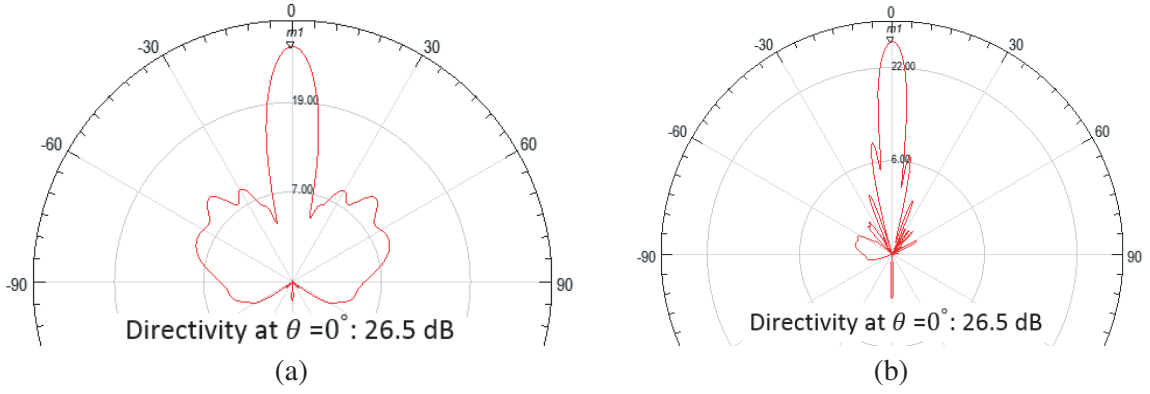
Figure 3. Two-dimensional antenna radiation pattern. (a) H-plane. (b) E-plane.
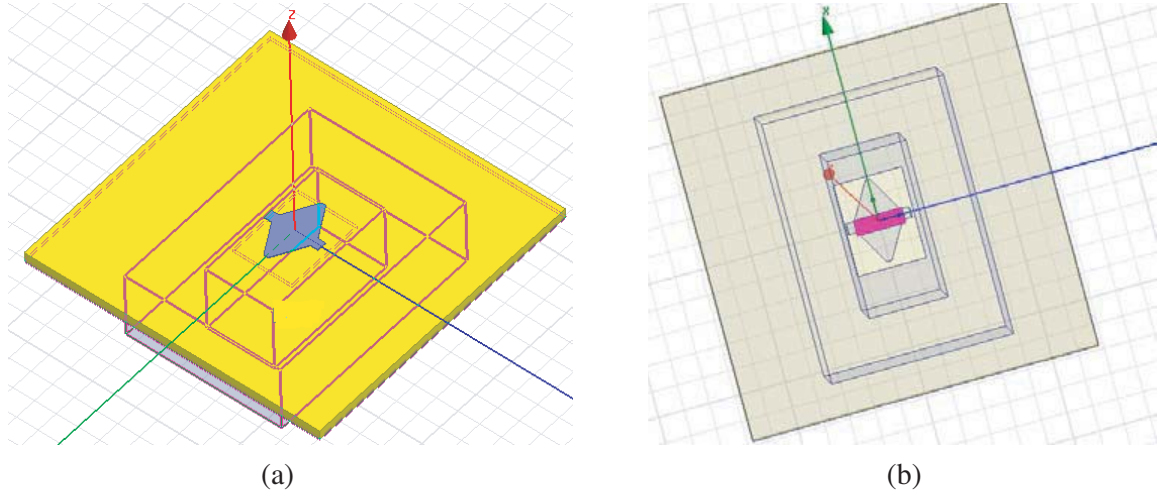

Figure 4. The antenna waveguide feed and its matching element. (a) Antenna waveguide feed structure. (b) Matching element of the waveguide feed.

with two R-L-C boundary ports with each placed in any side of the transition. For this modeling, ADS software has been implemented which equates the impedance values of S2p file with that of the parallel R-L-C lumped elements.

Equation (2) expresses the impedance of a parallel R-L-C lumped element as:

$$Z = \frac{1}{1/R + j\omega C - j/L\omega} \tag{2}$$

which can be reduced to:

$$Z = \frac{RL^2\omega^2}{R^2(LC\omega^2 - 1) + L^2\omega^2} + j\frac{R^2L\omega(1 - LC\omega^2)}{R^2(LC\omega^2 - 1) + L^2\omega^2} \tag{3}$$

It should be noted that there is a part in adjusting the section of a full wave simulator in which by inserting a lumped port and reading the equivalent impedance file in the form of SNP file, one can store the read file and insert it in an S2p file inside an ADS software. In this case to model the read impedance from an S2p file, one should equate it with that of a parallel RLC circuit whose component values can be tuned. In fact, having the real and imaginary parts of impedance from an S2p file at two frequency points and equating them with those given by Eq. (3), the values for R, L, and C will be obtained. In addition, two frequency points should be selected in such a way that the impedance and phase values of parallel R-L-C component are as close as possible to those of S2p file impedance. We

fed the input with a WR-12 waveguide port. Using these component values in a full wave simulator (ADS), in the form of R, L, and C boundary, we can estimate the second-order approximation of the impedance seen from two terminals of the whole antenna.

It should be noticed that the model is a two-degree model which means that the R-L-C impedance is a function of a two-dimensional antenna array at cut points. However, this is a nonlinear function which cannot be exactly modeled with R-L-C lumped elements with degree of two, so this is an approximation model. To have a more exact model, one should increase the degree of model with using more R-L-C components in a series and parallel combination. For example, with using a parallel R-L-C lumped ports series to parallel R-L-C lumped elements, the total degree for R-L-C components will be four.

The input port return loss 10 dB-bandwidth is more than 1 GHz. If we use the lumped port instead of R-L-C boundary, the power transmission factor from the input port to each lumped port will be equal to -4.02 dB. The phase difference between two ports is equal to $180°$ degrees.

Finally, with this R-L-C boundary modeling we could model the return loss of the final antenna with its waveguide to microstrip transition that helped us to match the input antenna waveguide.

6. FINAL ANTENNA WITH WAVEGUIDE FEED

By adding the waveguide to a two-dimensional array, the 3D pattern will have a null at its middle which shows that the final pattern is broadside. We also notice that the phase difference at the first two rows is exactly 180 degrees because of the waveguide structure. So, we rotated one side of the two-dimensional array by 180 degrees which generated 180 degrees positional phase difference and made the 180 degrees phase difference between the first two rows. Figure 5 demonstrates the final antenna array with its waveguide feed. The dimension of the final array, which contains 32×32 elements, is 38.1 mm × 37.4 mm.
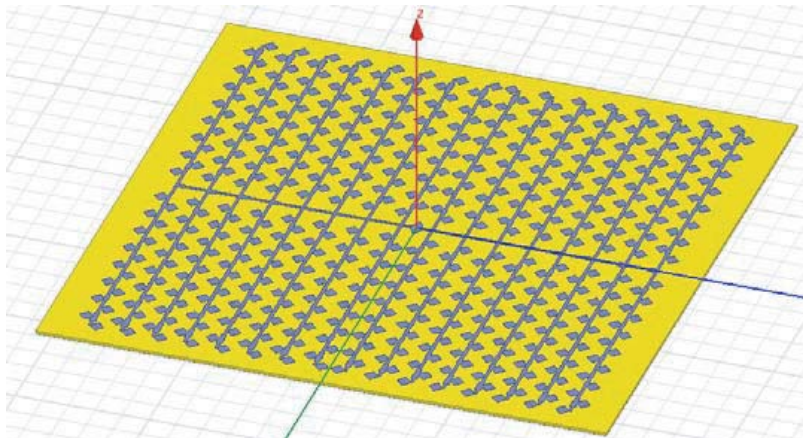

Figure 5. The final antenna array.

Finally, with proper waveguide shaping and tuning the size of its matching element, we could match the waveguide to the antenna. Figure 6 shows the normalized H- and E-plane directivity radiation patterns at 76.8 GHz with side lobe levels of -16.4 dB and -20.8 dB, respectively. Simulation results for directivity and realized gain at boreside is 26.6 dB and 24.6 dB at 76.8 GHz, respectively, which shows radiation efficiency of 63%. According to the real dimension of the array, which is $9.7\lambda \times 9.5\lambda$, the ideal directivity of a same aperture with uniform electrical field distribution is $D_{idl} = 4\pi A/\lambda^2 = 1158 = 30.6$ dB [16]. This value shows 4 dB drop in directivity, which shows 39.5% aperture efficiency for the proposed antenna array. It should be emphasized that this penalty in directivity is due to the field distribution on the elements, in order to reach the low side-lode level requirements, both in H- and E-planes.

The simulation result for reflection coefficient of the final antenna array from the waveguide port is -15 dB at 76.8 GHz as shown in Figure 7.
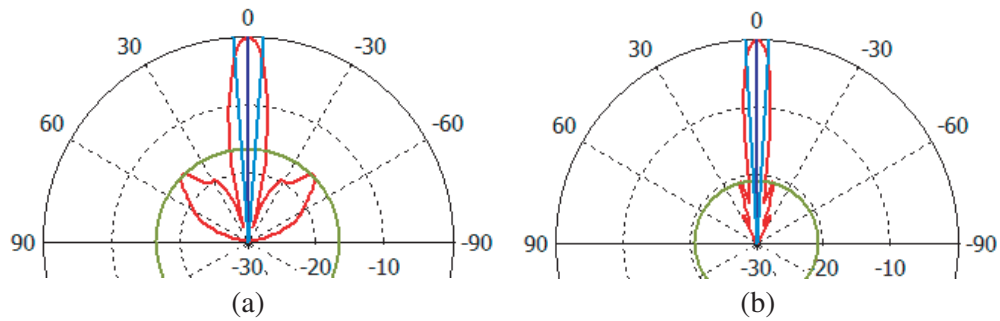
(a)   (b)

Figure 6. The directivity radiation pattern of the final antenna at 76.8 GHz. (a) H-plane. (b) E-plane.
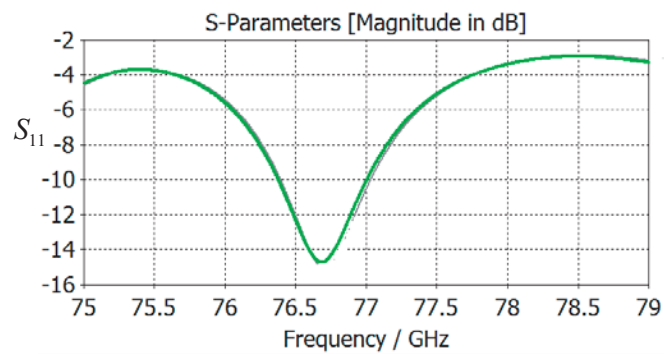

Figure 7. The simulated S_{11} for the final antenna array.

7. FABRICATION AND MEASUREMENT

The proposed antenna was fabricated on a Rogers RO4003 substrate using low-cost, single-layer standard PCB technology. Figure 8 shows a photograph of the manufactured antenna array. The radiation
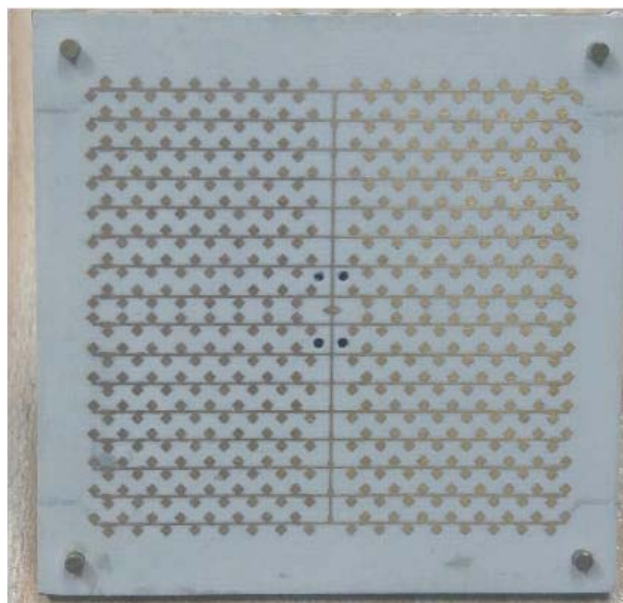

Figure 8. The photograph of the fabricated antenna.

(a) *H*-plane @ 76.4 GHz

(b) *E*-plane @ 76.4 GHz

(c) *H*-plane @ 76.8 GHz

(d) *H*-plane @ 76.8 GHz

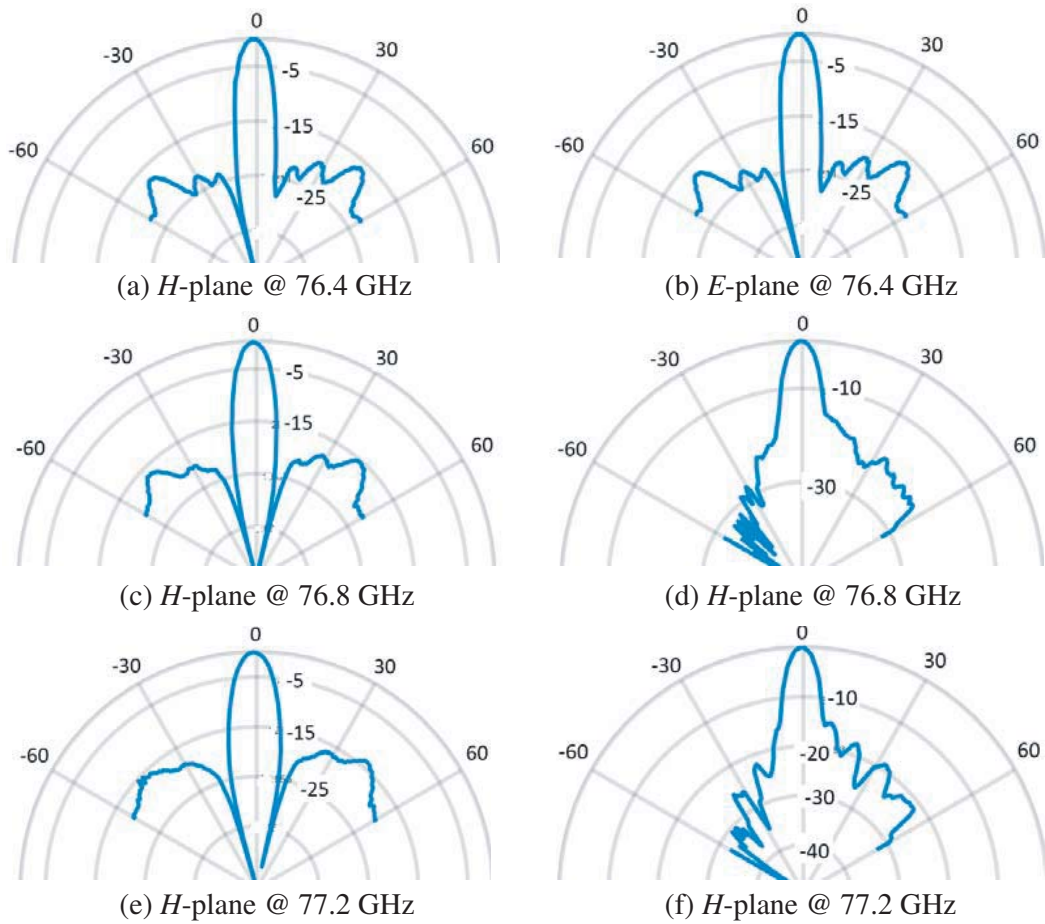(e) *H*-plane @ 77.2 GHz

(f) *H*-plane @ 77.2 GHz

Figure 9. The *H*-plane and *E*-plane radiation patterns of the manufactured 2D antenna array at (a), (b) 76.4, (c), (d) 76.8, and (e), (f) 77.2 GHz.
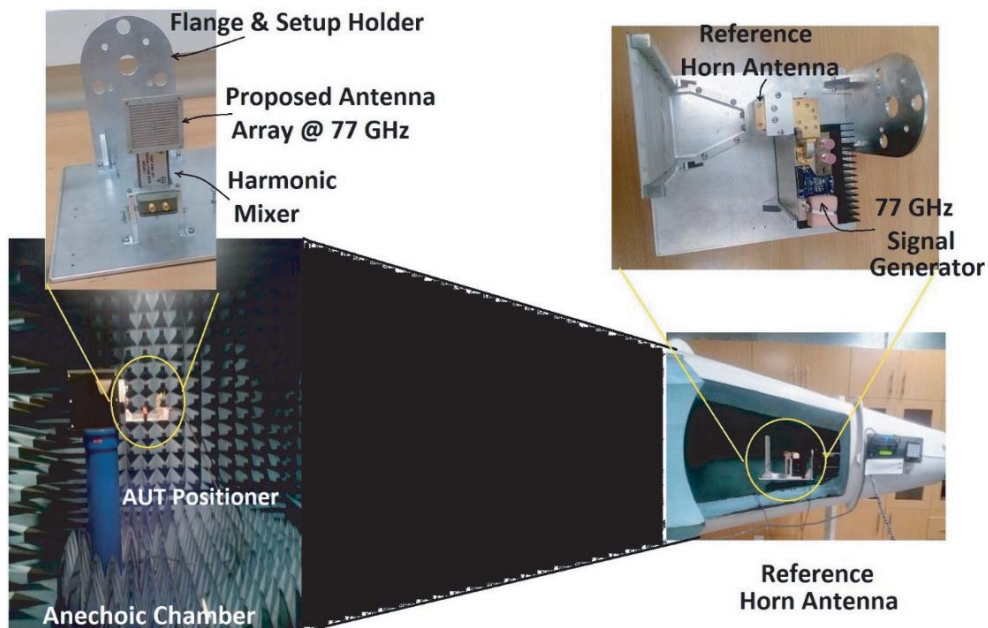

Figure 10. Measurement setup of the proposed Antenna Array in anechoic chamber.

pattern in both E-plane and H-plane at three different frequencies around 77 GHz were measured in an anechoic chamber and shown in Figure 9. Figure 10 shows the measurement setup in an anechoic chamber. In these measurements, a standard reference antenna with known gain was not available, and a lens loaded horn antenna, operating at 77 GHz, has been used as a reference transmitter, while the proposed antenna array acts as an under-test receiver antenna in the chamber. As can be seen from these figures, in H- and E-planes, the half power beamwidths are 6.8° and 8.7°, and the side lobe levels are better than -17 dB and -18 dB, respectively.

As the reference antenna with known gain was not available, the realized gain of the proposed antenna was not measured directly. But according to the measured half-power beamwidths in E- and H-planes, the measured gain is not less than $G_{meas} = \epsilon_{ap} 41,253/(\theta_E \cdot \theta_H) = 0.395 \times 697 = 275 = 24.4$ dB [16].

8. CONCLUSION

In this paper, an antenna was designed and completely simulated in full wave simulator. The simulated VSWR was better than 2 : 1 at the bandwidth of 1 GHz in the center frequency of 76.8 GHz, and the side lobe level was better than -17 dB. The realized gain of designed antenna was better than 24 dBi which corresponds to the radiation efficiency of 63 percent. The designed antenna was fabricated with low-cost single-layer standard PCB technology, and its radiation specifications were measured. The measured results were in good agreement with the simulated ones.

REFERENCES

1. Yasini, S. and K. Mohammadpour-Aghdam, "Design and simulation of a Comb-line fed microstrip antenna array with low side lobe level at 77 GHz for automotive collision avoidance radar," *IEEE Conf. MMWATT*, 87–90, Dec. 20–22, 2016.

2. Kolak, F. and C. Eswarappa, "A low profile 77 GHz three beam antenna for automotive radar," *2001 IEEE MTT-S Int. Microwave Sump. Dig.*, Vol. 2, 1107–1110, 2001.

3. Khalili, H., K. Mohammadpour-Aghdam, S. Alamdar, and M. Mohammad Taheri, "Low cost series-fed microstrip antenna arrays with extremely low side-lobe level," *IEEE Transactions on Antennas and Propagation*, Vol. 66, Vol. 9, Sep. 2018.

4. Peters, F. D. L., B. Boukari, S. O. Tatu, and T. A. Denidni, "77 GHz millimeter wave antenna array with Wilkinson diver feeding network," *Progress In Electromagnetics Research Letters*, Vol. 9, 193–199, 2009.

5. Chen, Z. and S. Otto, "A taper optimization for pattern synthesis of microstrip series-fed patch array antennas," *Proc. 2nd European Wireless Tech. Conference*, 160–163, Rome, Sep. 2009.

6. Benalla, A. and K. C. Gupta, "Design of a low side lobe short series-fed linear array of microstrip patches," *Electromagnetic Laboratory Scientific Report No. 93*, University of Colorado, Oct. 1987.

7. Otto, S., A. Rennings, O. Litschke, and K. Solbach, "A dual-frequency series-fed patch array antenna," *3rd European Conference on Antennas and Propagation*, 2009.

8. Bayderkhani, R. and H. R. Hassani, "Wideband and low side lobe slot antenna fed by series-fed printed array," *IEEE Trans. Antennas & Propagation*, Vol. 58, No. 12, Dec. 2010.

9. Ali, M. T., T. A. Rahman, M. R. Kamarudin, and M. N. Md Tan, "A planar antenna array with separated feed line for higher gain and sidelobe reduction," *Progress In Electromagnetic Research C*, Vol. 8, 69–82, 2009.

10. James, J. R. and P. S. Hall, *Handbook of Microstrip Antennas*, Peter Peregrinus, London, UK, 1989.

11. Iizuka, H., T. Watanabe, K. Sato, and K. Nishikawa, "Milimeter-wave microstrip line to waveguide transition fabricated on a single layer dielectric substrate," *IEICE Transactions on Communications*, Vol. 85, No. 6, 1169–1177, Jun. 2002.

12. Grabherr, W. and W. Menzel, "A new transition from microstrip line to rectangular waveguide," *22th European Microwave Conference Finland*, 1170–1175, Sep. 1992.

13. Grabherr, W., W. G. B. Huder, and W. Menzel, "Microstrip to waveguide transition compatible with mm-wave integrated circuits," *IEEE Transactions on Microwave Theory and Techniques*, Vol. 42, No. 9, 1842–1843, Sep. 1994.

14. Hyvonen, L. and A. Hujanen, "A compact MMIC-compatible microstrip to Waveguide transition," *IEEE MTT-S International Microwave Symposium*, Vol. 2, 875–878, Jun. 1996.

15. Morabito, A. F. and P. Rocca, "Reducing the number of elements in phase-only reconfigurable arrays generating sum and difference patterns," *IEEE Antennas and Wireless Propagation Letters*, Vol. 14, 1338–1341, 2015.

16. Hill, J. E., "Gain of directional antennas," *WJ Communication Edge White Paper*, Watkins-Johnson Company, Vol. 3, No. 4, Jul. 1976, reprinted 2001.